The Regioselectivity of Glutathione Adduct Formation with Flavonoid Quinone/Quinone Methides Is pH-Dependent

ARTICLE *in* CHEMICAL RESEARCH IN TOXICOLOGY · APRIL 2002

Impact Factor: 3.53 · DOI: 10.1021/tx010132l · Source: PubMed

6 AUTHORS, INCLUDING:

Hanem Awad
National Research Center, Egypt
44 PUBLICATIONS **763** CITATIONS
SEE PROFILE

Sjef Boeren
Wageningen University
124 PUBLICATIONS **3,881** CITATIONS
SEE PROFILE

Peter J van Bladeren
Nestlé S.A.
422 PUBLICATIONS **10,367** CITATIONS
SEE PROFILE

J.J.M. Vervoort
Wageningen University
398 PUBLICATIONS **7,795** CITATIONS
SEE PROFILE

The Regioselectivity of Glutathione Adduct Formation with Flavonoid Quinone/Quinone Methides Is pH-Dependent

Hanem M. Awad,[†,‡] Marelle G. Boersma,[†,§] Sjef Boeren,[†] Peter J. van Bladeren,[§,||] Jacques Vervoort,[†] and Ivonne M. C. M. Rietjens*[,§,||]

Laboratory of Biochemistry, Wageningen University, Dreijenlaan 3, 6703 HA Wageningen, The Netherlands, Department of Tanning Materials & Proteins, National Research Centre, 12622-Dokki, Cairo, Egypt, Division of Toxicology, Wageningen University, Tuinlaan 5, 6703 HE Wageningen, The Netherlands, and TNO/WU Centre for Food Toxicology, P.O. Box 8000, 6700 EA Wageningen, The Netherlands

Received August 8, 2001

In the present study, the formation of glutathionyl adducts from a series of 3′,4′-dihydroxy flavonoid *o*-quinone/*p*-quinone methides was investigated with special emphasis on the regioselectivity of the glutathione addition as a function of pH. The flavonoid *o*-quinones were generated using horseradish peroxidase, and upon purification by HPLC, the glutathionyl adducts were identified by LC/MS as well as ^{1}H and ^{13}C NMR. The major pH effect observed for the glutathione conjugation of taxifolin and luteolin quinone is on the rate of taxifolin and luteolin conversion and, as a result, on the ratio of mono- to diglutathione adduct formation. With fisetin, 3,3′,4′-trihydroxyflavone, and quercetin, decreasing the pH results in a pathway in which glutathionyl adduct formation occurs in the C ring of the flavonoid, being initiated by hydration of the quinone and H_2O adduct formation also in the C ring of the flavonoid. With increasing pH, for fisetin and 3,3′,4′-trihydroxyflavone glutathione adduct formation of the quinone occurs in the B ring at C2′ as the preferential site. For quercetin, the adduct formation of its quinone/quinone methide shifts from the C ring at pH 3.5, to the A ring at pH 7.0, to the B ring at pH 9.5, indicating a significant influence of the pH and deprotonation state on the chemical electrophilic behavior of quercetin quinone/quinone methide. Together the results of the present study elucidate the mechanism of the pH-dependent electrophilic behavior of B ring catechol flavonoids, which appears more straightforward than previously foreseen.

Introduction

Flavonoids are widely distributed in higher plants and form a natural component in the human diet. Recent interest in these substances has been stimulated by the potential health benefits arising from, among others, the anti-oxidant activity of these polyphenolic compounds (*1*). However, a number of studies have reported not only anti-oxidant (*2*−*9*) but also pro-oxidant (*10*−*12*) effects of the flavonoids. The most ubiquitous and widely studied flavonoid is quercetin, a B ring dihydroxylated flavonol. Some of its pro-oxidant properties have been attributed to the fact that it can undergo rapid autoxidation when dissolved in aqueous buffer at physiological pH. It has been observed that the rate of autoxidation for quercetin is highly pH-dependent and increases with increasing pH (*13*).

With respect to possible pro-oxidant toxicity, it is of interest to note that the mutagenic properties of the flavonoid quercetin, in a variety of bacterial and mammalian mutagenicity tests, have been related to its quinone/quinone methide pro-oxidant chemistry (Figure 1). Especially the electrophilicity of the *o*-quinone and quinone methide-type metabolites is of interest in the context of cytotoxicity, mutagenicity, and possible carcinogenicity (*3*). Identification of the oxidation products of quercetin and its analogues may therefore provide deeper insight into the mechanism of their toxic pro-oxidant action, and may form the basis for new biomarkers for

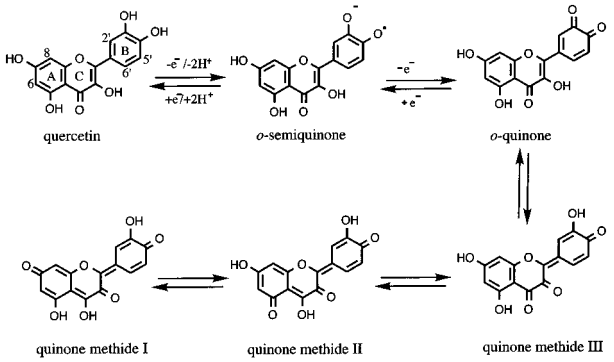

Figure 1. Schematic presentation of the formation of quercetin *o*-quinone and its isomerization to quercetin *p*-quinone methides, shifting the alkylating reactivity from the B to the A ring of quercetin. Quercetin = 3,5,7,3′,4′-pentahydroxyflavone, taxifolin lacks C2═C3, luteolin lacks C3−OH, and 3,3′,4′-trihydroxyflavone lacks C5−OH and C7−OH.

* Address correspondence to this author at the Division of Toxicology, Wageningen University, Tuinlaan 5, 6703 HE Wageningen, The Netherlands. Phone: 31-0317-482868. Fax: 31-0317-484801. E-mail: ivonne.rietjens@algemeen.tox.wau.nl.

† Laboratory of Biochemistry, Wageningen University.

‡ Department of Tanning Materials & Proteins, National Research Centre.

§ Division of Toxicology, Wageningen University.

|| TNO/WU Centre for Food Toxicology.

10.1021/tx010132l CCC: $22.00
Published on Web 02/22/2002

the detection of pro-oxidant activity of flavonoids. Previous studies that included incubating flavonoids with peroxidases in the presence of GSH have indicated the capacity of GSH to scavenge the flavonoid semiquinone radical, thereby regenerating the flavonoid and generating GSSG and reactive oxygen species leading to toxicity (*12*, *14*). This reaction appeared to be especially efficient for flavones and flavanones containing a phenol-type substituent pattern in their B ring (*14*, *15*). The GSH-oxidizing pro-oxidant activity of this type of flavones and flavanones seemed to partly correlate with the high one-electron redox potential of the corresponding phenoxyl radicals (*14*, *16*). Flavonoids containing a catechol-type substituent pattern in their B ring did not co-oxidize GSH when oxidized by horseradish peroxidase (HRP), presumably because of their lower one-electron redox potentials. Instead, GSH conjugate formation involving their *o*-quinone/quinone methide metabolites was observed (*17*−*20*).

We have recently investigated the quinone/quinone methide chemistry of a series of 3′,4′-dihydroxyflavones at pH 7.0 and identified their adducts using the glutathione (GSH) trapping method (*18*). Results obtained revealed that, especially for fisetin, the regioselectivity and the nature of the quinone adducts formed appear to be dependent on the pH. With decreasing pH, the site of GSH adduct formation shifted from the B to the C ring (*18*). The objective of the present study was to further investigate the mechanism of the pH-dependent chemistry of flavonoid quinone/quinone methides. Thus, the pH-dependent quinone/quinone methide chemistry of quercetin, taxifolin, luteolin, and 3,3′,4′-trihydroxyflavone was investigated, using the GSH trapping method, HPLC, ^{1}H and ^{13}C NMR, and LC/MS analysis to identify the glutathionyl adducts.

Materials and Methods

Materials. Quercetin was obtained from Acros Organics (NJ). Fisetin was from Aldrich (Steinheim, Germany). Luteolin and 3,3′,4′-trihydroxyflavone were from Indofine (Somerville). Taxifolin was obtained from ICN Biomedicals Inc. (OH). Horseradish peroxidase (HRP) was obtained from Boehringer (Mannheim, Germany). Glutathione, reduced form, was purchased from Sigma (St. Louis, MO). All substrates were of 98−99% purity. Hydrogen peroxide, potassium hydrogen phosphate, potassium dihydrogen phosphate, citric acid, trisodium citrate dihydrate, anhydrous sodium carbonate, sodium hydrogen carbonate, and trifluoroacetic acid were purchased from Merck (Darmstadt, Germany). Deuterium oxide was obtained from ARC Laboratories (Amsterdam, The Netherlands). Acetonitrile and methanol were HPLC-grade from Lab-Scan, Analytical Sciences (Dublin, Ireland).

pH-Dependent Incubation of Flavonoids with Glutathione. To a starting solution of flavonoid (final concentration 150 μM added from a 10 mM stock solution in methanol) in 25 mM citrate, phosphate, or carbonate, depending on the pH which varied between 3.5 and 11.0 (prepared according to literature) (*21*−*30*), containing GSH (final concentration 1.0 mM) was added HRP to a final concentration of 0.1 μM, followed by addition of H_2O_2 (final concentration of 200 μM added from a 20 mM stock solution in water). Upon 8 min incubation at 25 °C, the incubation mixture was analyzed by HPLC.

Analytical High-Performance Liquid Chromatography. HPLC was performed with a Waters M600 liquid chromatography system. Analytical separations were achieved using an Alltima C18 column (4.6 × 150 mm) (Alltech, Breda, The Netherlands). The column was eluted at 0.7 mL/min with water containing 0.1% (v/v) trifluoroacetic acid. A linear gradient from 0% to 30% acetonitrile in 18 min was applied, followed by 2 min isocratic elution with 30% acetonitrile. Hereafter a linear gradient from 30% to 100% acetonitrile was used in 10 min. The percentage of acetonitrile was kept at 100% for another 10 min. An injection loop of 10 μL was used. Detection was carried out with a Waters 996 photodiode array detector measuring spectra between 200 and 450 nm. Chromatograms presented are based on detection at 290 nm. Product peaks were collected and freeze-dried for further analysis by NMR and LC/MS. Freeze-dried samples were dissolved in 25 mM buffer, made with deuterated water when samples were used for NMR analysis.

NMR Measurements. ^{1}H and ^{13}C NMR measurements were performed on a Bruker DPX 400 or Bruker AMX 500 spectrometer. For ^{1}H NMR measurements 1.5 s presaturation delay was used with a 70° pulse angle and a 2.2 s acquisition time (7575 Hz sweep width, 32K data points). The temperature was 7 °C. The data were processed using an exponential multiplication of 0.5 or 1.0 Hz and zero-filling to 64K data points. Resonances are reported relative to HDO at 4.79 ppm. ^{13}C NMR measurements were performed in deuterated methanol/D_2O at 15 °C with a dedicated 5 mm ^{13}C NMR probe (32 000 Hz sweep width, 64K data points, 28 000 scans).

Liquid Chromatography/Mass Spectrometry. LC/MS analysis was performed to further characterize the peaks in the HPLC elution pattern. An injection volume of 10 μL from the incubation mixture or from the purified metabolite dissolved in buffer was used, and separation of the products was achieved on a 4.6 × 150 mm Alltima C18 column (Alltech, Breda, The Netherlands). A gradient from 10% to 30% acetonitrile in water containing 0.1% (v/v) trifluoroacetic acid was applied at a flow rate of 0.7 mL/min in 13 min. The percentage of acetonitrile was kept at 30% for 2 min and then increased to 100% in another 2 min. Mass spectrometric analysis (Finnigan MAT 95, San Jose, CA) was performed in the positive electrospray mode using a spray voltage of 4.5 kV and a capillary temperature of 180 °C with nitrogen as sheath and auxiliary gas.

Results

pH-Dependent Formation of Glutathionyl Taxifolin Adducts. Figure 2a−c shows the pH-dependent formation of the glutathionyl taxifolin adducts. At pH 7.0 (Figure 2b), two major peaks are observed with retention times of 20.4 and 22.3 min. The first peak was identified previously as 2′,5′-diglutathionyl taxifolin and the second peak as a mixture of 2′- and 5′-glutathionyl taxifolin (*18*). Table 1 shows the UV absorption maxima for these glutathionyl taxifolin adducts. With pH values increasing from 3.5 to 7.0 to 10.5 (Figure 2a−c), the peak intensity of the 2′,5′-diglutathionyl adduct decreases, and a lower extent of taxifolin conversion is observed. This is in line with previous observations that formation of diglutathionyl flavonoid adducts starts to occur when the monoadduct, because of its concentration and reactivity, starts to compete as a substrate with the parent flavonoid. At pH 10.5 (Figure 2c), metabolite formation was no longer significant. Thus, the major effect of increasing pH on HRP-mediated taxifolin GSH conjugation is on the rate of taxifolin conversion and, as a result, the ratio of mono- to diglutathionyl adduct formation.

pH-Dependent Formation of Glutathionyl Luteolin Adducts. Figure 3a−c shows the pH-dependent formation of the glutathionyl luteolin adducts. At pH 7.0 (Figure 3b), two metabolites with retention times of 22.7 and 25.0 min can be detected which were identified previously as 2′,5′-diglutathionyl and 2′-glutathionyl luteolin (*18*). Table 1 shows the UV absorption maxima for these glutathionyl luteolin adducts. Going from pH 3.5 to 11.0 (Figure 3a−c), the ratio between these two

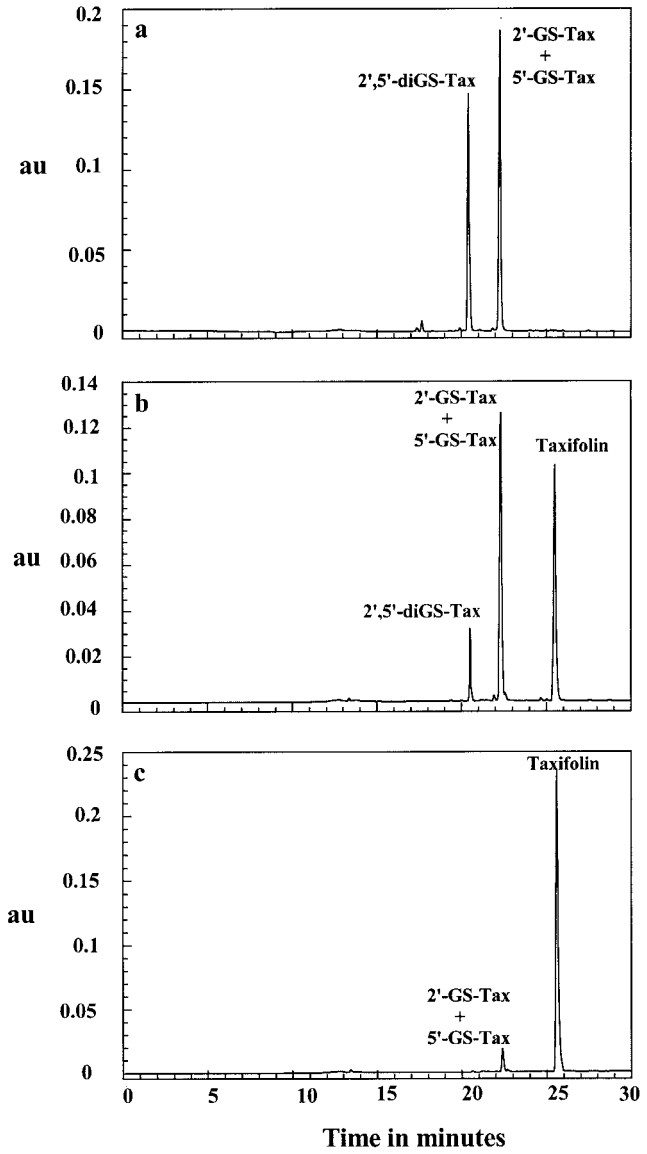

Figure 2. HPLC chromatograms of the incubation of taxifolin with HRP in the presence of GSH at (a) pH 3.5, (b) pH 7.0, and (c) pH 10.5.

metabolites shifts in favor of the monoadduct due to a decreased overall luteolin conversion. This result is in line with what is observed for the pH-dependent effect on taxifolin quinone chemistry.

pH-Dependent Formation of Glutathionyl Quercetin Adducts. Figure 4a−d shows the pH-dependent formation of glutathionyl quercetin adducts. At pH 7.0 (Figure 4b), the formation of two major metabolites with retention times of 17.1 and 18.1 min, identified previously as 8-glutathionyl and 6-glutathionyl quercetin (*19*, *20*), is observed. The LC/MS spectra of these peaks obtained with the relatively soft electrospray ionization show, in contrast to previous more harsh ionized MALDI-TOF mass spectra, that the 8- and 6-glutathionyl adducts are present in their hydrated forms with M + 1 peaks at *m*/*z* 626.0. The occurrence of the water addition in the two metabolites clearly follows from the LC/MS analysis, and may result from a peroxidase/H_2O_2-catalyzed reaction resulting in water addition as reported in the literature (*24*). The UV spectra of the hydrated 6-glutathionyl and the 8-glutathionyl quercetin adducts reveal a shift in their UV absorption maxima from 370.1 to 295.1 and 299.9 nm, respectively, reflecting the loss of the conjugation between the ketone of the C ring and B ring (Table 1) (*17*, *25*). The peak intensities of these 6-glutathionyl and 8-glutathionyl quercetin metabolites decrease with increasing pH (Figure 4c,d). This is accompanied by the formation of at least two new metabolites with retention times of 21.5 and 23.8 min. At pH ≥9.5, the hydrated 6-glutathionyl and 8-glutathionyl quercetin adducts are no longer observed, and the two new metabolites become the major ones (Figure 4d). Table 1 shows the UV absorption maxima for these glutathionyl adducts. LC/MS analysis of these metabolites with retention times of 21.5 and 23.8 min reveals M + 1 peaks at *m*/*z* 913.0 and 1218.0, respectively. This indicates the formation of a di- and a triglutathionyl quercetin adduct, respectively. Table 2 shows the ^{1}H NMR characteristics of these two major metabolites collected from HPLC. Comparison of the ^{1}H NMR data of these two metabolites to those of quercetin (Table 2) (*19*, *20*, *26*−*28*) reveals the loss of the H2′ and H5′ signals as well as the loss of the $^4J_{H2'-H6'}$ coupling of 2.1 Hz and the $^3J_{H5'-H6'}$ coupling of 8.5 Hz for the H6′ for the diglutathionyl adduct. For the triglutathionyl adduct, the ^{1}H NMR data indicate the loss of the H2′, H5′, and H6′ signals. In addition to the aromatic ^{1}H resonances, the ^{1}H NMR spectra of the two adducts show the ^{1}H NMR resonances of the glutathionyl side chain. On the basis of these ^{1}H NMR characteristics and LC/MS data, the two metabolites can be identified as 2′,5′-diglutathionyl quercetin and 2′,5′,6′-triglutathionyl quercetin resulting from conjugation in the B ring instead of in the A ring. This glutathionyl addition in the B ring is not accompanied by hydration since the *m*/*z* signals exactly match the di- and triglutathionyl adducts. At pH values <7.0, two major peaks with almost the same retention times as the hydrated 6-glutathionyl and 8-glutathionyl quercetin metabolites are observed (Figure 4a). Surprisingly, however, the ^{1}H NMR spectra of these two metabolites are different from those of the metabolites formed at pH 7.0 (Figure 5). The ^{1}H NMR spectra reveal the retention of all the parent compound aromatic protons in both metabolites formed at pH 3.5, including the protons at C2′, C5′, and C6′ (B ring) and at C6 and C8 (A ring) (Figure 5a,b) (Table 2) (*19*, *20*, *26*−*28*). In addition to the aromatic ^{1}H resonances, the ^{1}H NMR

Table 1. UV Absorption Maxima for the Investigated Flavonoids and Their Adducts in A, B, and C Rings

compound	λ_{max} (nm)
taxifolin	290.4
2′-glutathionyl taxifolin	295.1
5′-glutathionyl taxifolin	290.4
2′,5′-diglutathionyl taxifolin	285.6
luteolin	252.5 and 347.6
2′-glutathionyl luteolin	257.2 and 328.5
2′,5′-diglutathionyl luteolin	261.9 and 328.5
quercetin	252.6 and 370.1
6-glutathionyl quercetin	295.1
8-glutathionyl quercetin	299.9
2′,5′-diglutathionyl quercetin	252.5, 304.6, and 347.6
2′,5′,6′-triglutathionyl quercetin	252.5 and 347.6
2-GS-Q-a	295.1
2-GS-Q-b	295.1
3,3′,4′-trihydroxyflavone	247.7 and 361.1
2′-glutathionyl 3,3′,4′-trihydroxyflavone	257.2, 285.6, and 352.4
2′,5′-diglutathionyl 3,3′,4′-trihydroxyflavone	233.6, 280.9, and 333.3
2-GS-3,3′,4′-tri-OH-flavone-a	257.2 and 280.9
2-GS-3,3′,4′-tri-OH-flavone-b	257.2 and 280.9

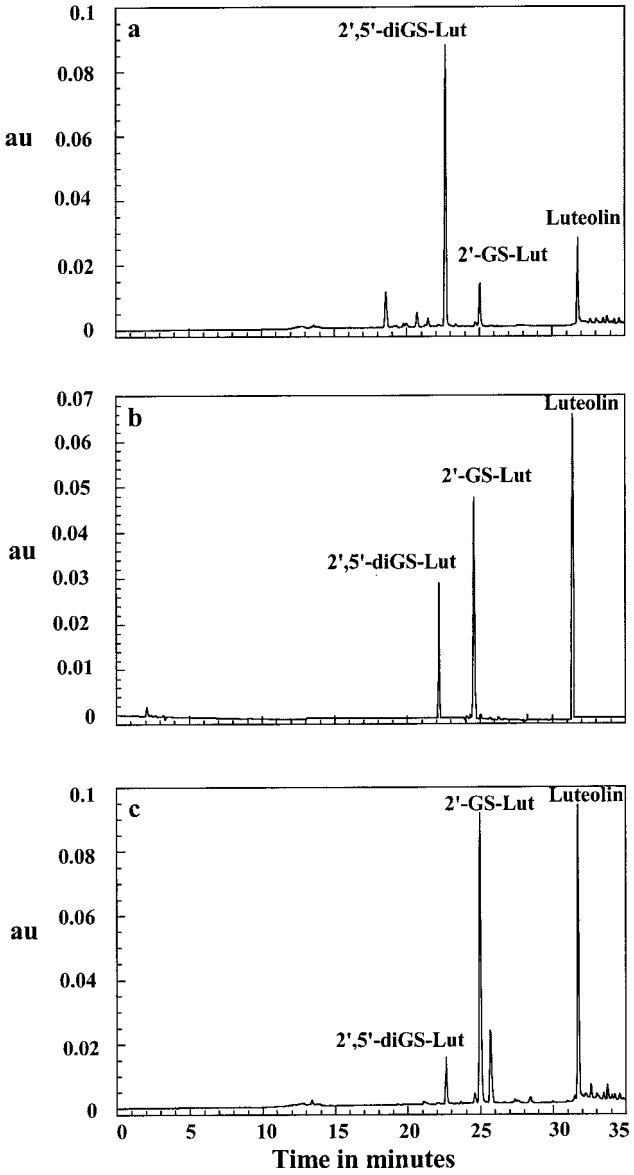

Figure 3. HPLC chromatograms of the incubation of luteolin with HRP in the presence of GSH at (a) pH 3.5, (b) pH 7.0, and (c) pH 11.0.

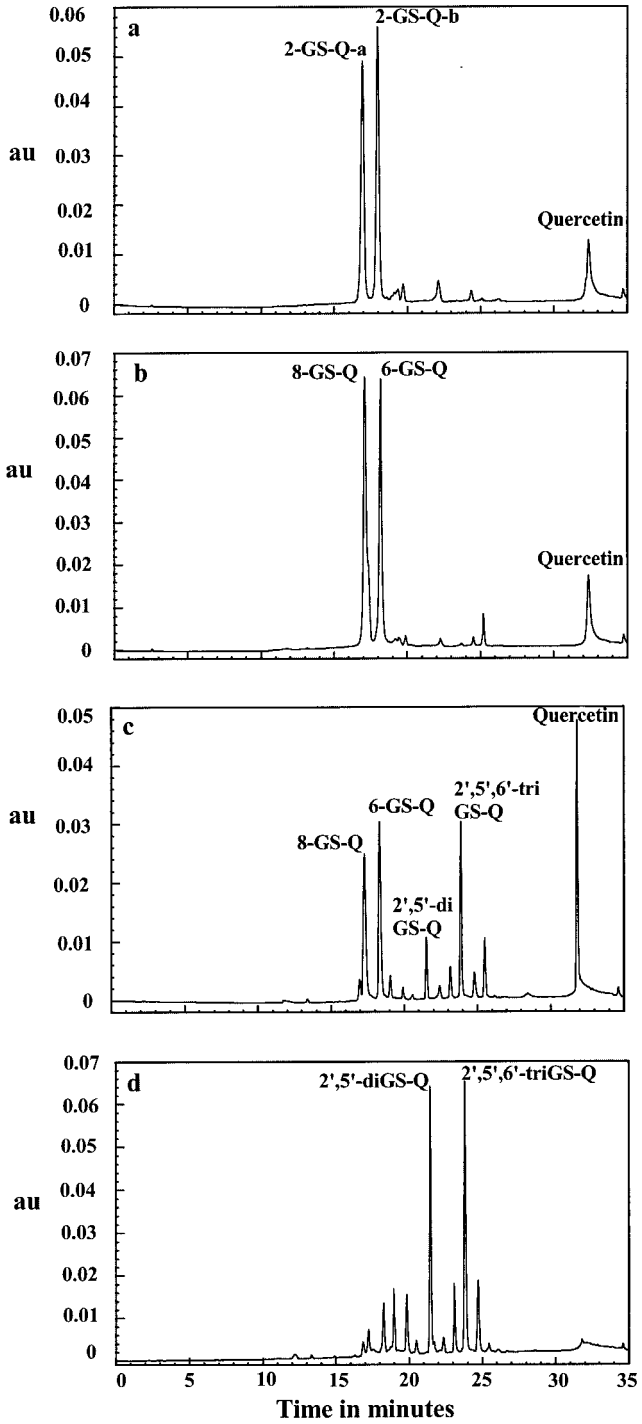

Figure 4. HPLC chromatograms of the incubation of quercetin with HRP in the presence of GSH at (a) pH 3.5, (b) pH 7.0, (c) pH 8.5, and (d) pH 9.5.

spectra of the two adducts show the ^{1}H NMR resonances of the glutathionyl side chain. LC/MS analysis of the purified metabolites shows an M + 1 peak for both metabolites at *m/z* 626.0. Because the *m/z* value expected for protonated monoglutathionyl quercetin equals *m/z* 608.0, the observation of a peak at *m/z* 626.0 for both metabolites points to formation of monoglutathionyl adducts which contain an additional H_2O molecule. The UV spectra of these adducts reveal an absorbance peak at 295.1 nm for both metabolites and disappearance of the absorbance peak at 370.1 nm for quercetin (Table 1), indicating the loss of conjugation between the A ring and the B ring (*17*, *25*). ^{13}C NMR spectra of the two purified metabolites (Figure 6, Table 3) reveal formation of two ^{13}C resonances at 92.5 and 99.2 ppm for the metabolite with a retention time of 17.1 min and at 90.4 and 94.6 ppm for the metabolite with a retention time of 18.1 min which can be assigned to the two sp^3-hybridized C atoms at C2 and C3. In addition, the ^{13}C NMR spectra of the metabolites each reveal only one resonance in the carbonyl region (at 192.0 ppm and at 190.0 ppm, respectively), indicating the presence of only one carbonyl group for each metabolite. Together these data point to glutathionyl adduct formation accompanied by H_2O adduct formation, both at the C ring of the quercetin *o*-quinone/quinone methide, similar to what was recently observed for fisetin at low pH values (*18*) and in agreement with the reported literature (*28*) (see Discussion). The fact that two metabolites with similar MS, UV, ^{1}H NMR, and ^{13}C NMR characteristics are observed points to the formation of different (diastereo) isomers of these combined H_2O/glutathionyl adducts.

Altogether the adduct formation of quercetin quinone/quinone methide shifts from the C ring at pH 3.5, to the

Table 2. ^{1}H NMR Resonances and Coupling Constants of the Glutathionyl Adducts of Quercetin, Labeled 2-GS-Q-a, 2-GS-Q-b, 2′,5′-diGS-Q, and 2′,5′,6′-triGS-Q, Isolated from HPLC (Figure 4)

	2-GS-Q-a		2-GS-Q-b		2′,5′-diGS-Q		2′,5′,6′-triGS-Q	
	chemical shift (ppm)	coupling constant (Hz)	chemical shift (ppm)	coupling constant (Hz)	chemical shift (ppm)	coupling constant (Hz)	chemical shift (ppm)	coupling constant (Hz)
H6	5.96 (d)	$^4J_{H6-H8} = 2.4$	5.99 (d)	$^4J_{H6-H8} = 2.4$	6.10 (d)	$^4J_{H6-H8} = 2.1$	6.00 (d)	$^4J_{H6-H8} = 2.1$
H8	6.00 (d)	$^4J_{H8-H6} = 2.4$	6.15 (d)	$^4J_{H8-H6} = 2.4$	6.21 (d)	$^4J_{H8-H6} = 2.1$	6.20 (d)	$^4J_{H8-H6} = 2.1$
H5′	6.77 (d)	$^3J_{H5'-H6'} = 8.4$	6.72 (d)	$^3J_{H5'-H6'} = 8.4$	–	–	–	–
H6′	7.18 (dd)	$^3J_{H6'-H5'} = 8.4$	7.15(dd)	$^3J_{H6'-H5'} = 8.4$	6.90 (s)	–	–	–
		$^4J_{H6'-H2'} = 2.4$		$^4J_{H6'-H2'} = 2.4$		–		–
H2′	7.26 (d)	$^4J_{H2'-H6'} = 2.4$	7.22 (d)	$^4J_{H2'-H6'} = 2.4$	–	–	–	–
Glu Hβ	1.75 (m)		1.82 (m)		1.55 (m)		1.45 (m)	
					1.69 (m)		1.54 (m)	
							1.67 (m)	
Glu Hγ	2.04 (m)		2.17 (m)		1.87 (m)		1.75 (m)	
					2.11 (m)		1.86 (m)	
							1.99 (m)	
Cys Hβ1	2.45 (dd)		2.31 (dd)		2.65 (dd)		2.15 (dd)	
					2.88 (dd)		2.67 (dd)	
							2.97 (dd)	
Cys Hβ2	2.59 (dd)		2.74 (dd)		3.10 (dd)		3.00 (dd)	
					3.16 (dd)		3.10 (dd)	
							3.25 (dd)	
Gly Hα1	3.48 (d)		3.55 (d)		3.45 (d)		3.49 (d)	
Gly Hα2	3.53 (d)		3.55 (d)		3.49 (d)		3.49 (d)	
Glu-Hα	3.45 (t)		3.51 (m)		3.23 (t)		3.35 (m)	
					3.28 (t)			
Cys Hα	3.99 (dd)		3.78 (dd)		3.81 (dd)		3.85 (dd)	
					3.19 (m)		3.99 (dd)	
							4.10 (dd)	

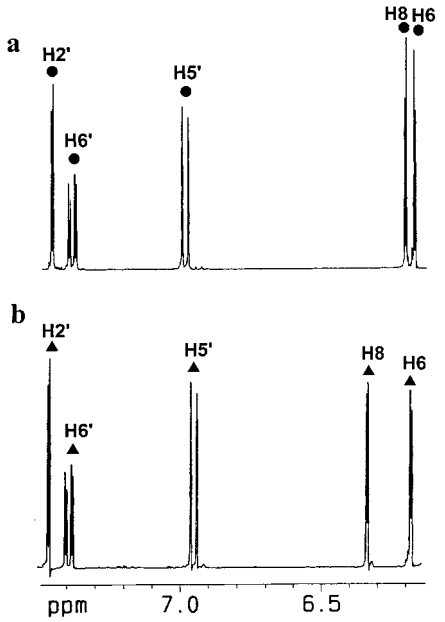

Figure 5. Aromatic parts of the ^{1}H NMR spectra of the two glutathionyl metabolites, 2-GS-Q-a (a) and 2-GS-Q-b (b), formed in the incubation of quercetin with HRP in the presence of GSH at pH <7.0, both measured in 25 mM sodium citrate (pD = 3.5) in D_2O.

A ring at pH 7.0, to the B ring at pH 9.5, indicating a significant influence of the pH on the regioselectivity of glutathione conjugation to quercetin quinone/quinone methide.

pH-Dependent Formation of Glutathionyl 3,3′,4′-Trihydroxyflavone Adducts. Figure 7a−d shows the pH-dependent formation of the glutathionyl 3,3′,4′-trihydroxyflavone adducts. At pH 7.0 (Figure 7c), only one major metabolite with a retention time of 23.7 min can be detected, which was identified previously as 2′-glutathionyl 3,3′,4′-trihydroxyflavone (*18*). At pH >7.0, formation of a second major metabolite was observed with a retention time at 22.0 min (Figure 7d). LC/MS analysis of this purified metabolite reveals a M + 1 peak at *m*/*z* 881.0. This indicates the formation of a diglutathionyl adduct. Table 1 shows the UV absorption maxima for these glutathionyl adducts of 3,3′,4′-trihydroxyflavone. Table 4 shows the ^{1}H NMR characteristics of this major metabolite collected from HPLC. Comparison of the ^{1}H NMR data of this metabolite to those of 3,3′,4′-trihydroxyflavone (Table 4) (*18*, *26*, *29*) reveals the loss of the H2′ and H5′ signals as well as the loss of the $^4J_{H2'-H6'}$ coupling of 1.4 Hz and the $^3J_{H5'-H6'}$ coupling of 8.5 Hz for the H6′ signal. In addition to the aromatic ^{1}H resonances, the ^{1}H NMR spectrum of the adduct shows the ^{1}H NMR resonances of the glutathionyl side chain. On the basis of these ^{1}H NMR characteristics and LC/MS data, this metabolite can be identified as 2′,5′-diglutathionyl 3,3′,4′-trihydroxyflavone. At pH values <7.0, the peak intensity of the 2′-glutathionyl adduct decreases with decreasing pH values, and the formation of two new major metabolites with retention times of 18.8 and 19.8 min can be observed. At very low pH values, the 2′-glutathionyl adduct is no longer observed, and the two new metabolites become the major metabolites detected (Figure 7a). ^{1}H NMR spectra of these two major metabolites of 3,3′,4′-trihydroxyflavone collected from HPLC with retention times of 18.8 and 19.8 min (Figure 7a) reveal the retention of all parent compound aromatic protons in both adducts (Table 4). This indicates the formation of glutathionyl 3,3′,4′-trihydroxyflavone adducts at other positions than C2′, C5′, and C6′ (B ring) or C5, C6, C7, and C8 (A ring) (Table 4) (*26*, *29*). The UV spectra of these adducts reveal an absorbance peak at 280.9 nm for both metabolites and disappearance of the absorbance peak at 361.1 nm for 3,3′,4′-trihydroxyflavone (Table 1), indicating the loss of conjugation between the A ring and B ring (*17*, *25*). LC/MS analysis of these two purified metabolites reveals a M + 1 peak for both metabolites at *m*/*z* 594.0. Because the *m*/*z* value expected for protonated monoglutathionyl 3,3′,4′-trihydroxyflavone equals

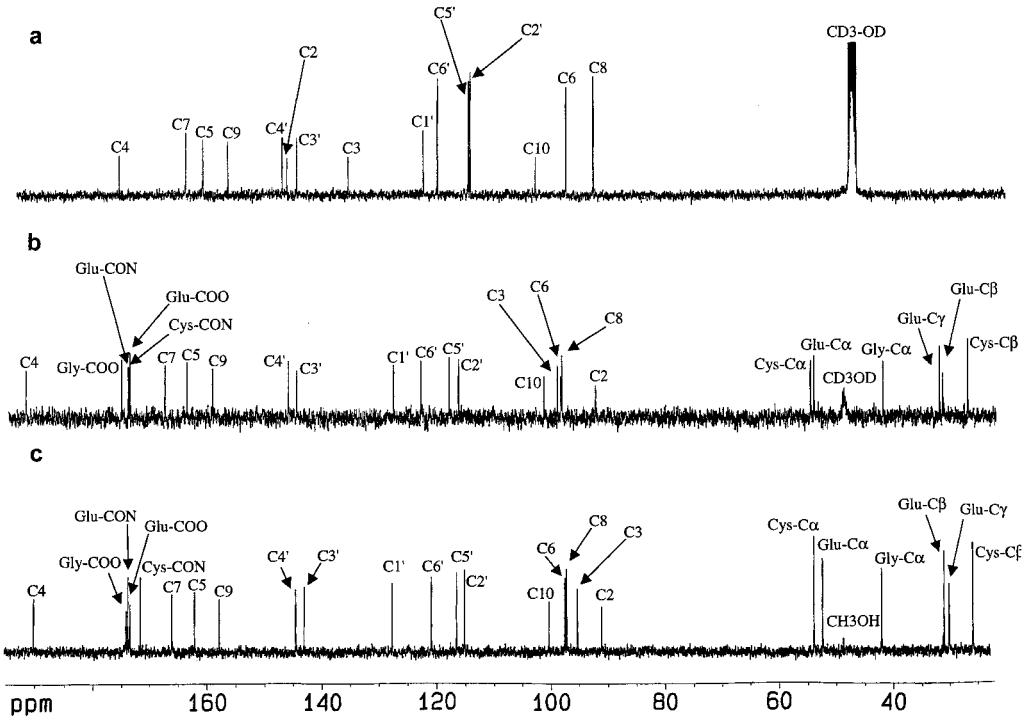

Figure 6. ^{13}C NMR spectra of (a) quercetin and the two glutathionyl metabolites in the C ring, 2-GS-Q-a (b) and 2-GS-Q-b (c), formed in the incubation of quercetin with HRP in the presence of GSH at pH <7.0.

Table 3. ^{13}C NMR Chemical Shifts of Quercetin and the C Ring Glutathionyl Adducts of Quercetin Labeled 2-GS-Q-a and 2-GS-Q-b

	chemical shift (ppm)		
	quercetin	2-GS-Q-a	2-GS-Q-b
C2	147.4	92.5	90.4
C3	136.7	99.2	94.6
C4	176.7	192.0	190.0
C5	161.9	163.8	161.7
C6	98.6	98.6	96.8
C7	165.0	167.7	165.6
C8	93.8	98.5	96.5
C9	157.6	159.4	157.4
C10	103.9	101.6	99.7
C1′	123.5	127.8	127.1
C2′	115.4	116.5	114.5
C3′	145.6	144.7	142.5
C4′	148.2	146.1	144.0
C5′	115.6	118.2	115.9
C6′	121.1	123.0	120.3
Cys Cβ	–	27.2	25.1
Glu Cβ	–	31.6	29.3
Glu Cγ	–	32.2	30.2
Gly Cα	–	42.2	41.3
Glu Cα	–	54.3	51.7
Cys Cα	–	54.9	53.2
Cys CON	–	173.8	171.2
Glu COO	–	173.8	173.0
Glu CON	–	174.1	173.4
Gly COO	–	175.3	173.7

576.0, the observation of a peak at *m*/*z* 594.0 for both metabolites points to formation of monoglutathionyl adducts which contain an additional H_2O molecule. Together these data point to glutathionyl adduct formation accompanied by H_2O adduct formation, both at the C ring of the 3,3′,4′-trihydroxyflavone *o*-quinone/quinone methide, similar to what was observed for fisetin (*18*, *28*) and quercetin (above). The fact that two metabolites with similar MS and ^1H NMR characteristics are observed points to formation of different (diastereo)isomers of these combined H_2O/glutathionyl adducts. Together these results point to a reaction of the quinone/quinone methide of 3,3′,4′-trihydroxyflavone with glutathione which is similar to the reaction of fisetin with glutathione discussed previously (*18*, *28*) and with quercetin (above).

Identification of the Flavonoid Diglutathionyl Adducts. The identification of the diglutathionyl B ring adducts was generally based on the assumption that the remaining singlets in the ^1H NMR spectra pertain to H6′ (Tables 2 and 4). However, since all B ring proton resonances are close, in theory this single resonance may be ascribed to all three B ring protons, indicating formation of 2′,5′- or 2′,6′- or 5′,6′-diglutathionyl adducts. Therefore, additional experiments were performed in which the 2′-glutathionyl adducts of the studied flavonoids were incubated with HRP/H_2O_2 in the presence of GSH. This resulted in the formation of metabolites with the same retention times, the same UV spectra, the same mass, and the same ^1H NMR spectra as the compounds identified as the 2′,5′-diglutathionyl adducts. The formation of these products from the 2′-glutathionyl adducts eliminates the possibility of their identification as 5′,6′-diglutathionyl adducts. Nevertheless, their formation from 2′-glutathionyl conjugates may still point at either the 2′,5′- or the 2′,6′-diglutathionyl adducts. Unfortunately, like the H5′ and H6′ resonances in ^1H NMR, also the C5′ and C6′ ^{13}C resonances (see, for example, Figure 6) appear too close to provide the possibility for unequivocal discrimination of the presence of either a C5′-H5′ or a C6′-H6′ in the diadducts by, for example, a 2D ^1H-^{13}C-correlation spectrum. However, previous studies with taxifolin have unequivocally demonstrated the 2′ and 5′ as the most reactive sites in the B ring quinone reflected by formation of 2′-mono and 5′-mono- but not a 6′-monoglutathionyl taxifolin metabolite (*18*). Furthermore, adduct formation at C6′ can be expected to be hampered by steric hindrance. Since for taxifolin isolation of a 5′-monoglutathionyl adduct was

Table 4. ^{1}H NMR Resonances and Coupling Constants of the Glutathionyl Adducts of 3,3′,4′-Trihydroxyflavone, Labeled 2-GS-3,3′,4′-tri-OH-flavone-a, 2-GS-3,3′,4′-tri-OH-flavone-b, and 2′,5′-diGS-3,3′,4′-tri-OH-flavone, Isolated from HPLC (Figure 6)

	2-GS-3,3′,4′-tri-OH-flavone-a		2-GS-3,3′,4′-tri-OH-flavone-b		2′,5′-diGS-3,3′,4′-tri-OH-flavone	
	chemical shift (ppm)	coupling constant (Hz)	chemical shift (ppm)	coupling constant (Hz)	chemical shift (ppm)	coupling constant (Hz)
H5′	6.79 (d)	$^3J_{H5'-H6'} = 8.4$	6.74 (d)	$^3J_{H5'-H6'} = 8.4$	–	–
H8	7.01 (dd)	$^4J_{H8-H6} = 1.0$ $^3J_{H8-H7} = 8.8$	7.18 (dd)	$^4J_{H8-H6} = 1.0$ $^3J_{H8-H7} = 8.4$	7.43 (dd)	$^4J_{H8-H6} = 1.0$ $^3J_{H8-H7} = 8.4$
H6	7.05 (tr)	$^4J_{H6-H8} = 1.0$ $^3J_{H6-H7} = 6.9$ $^3J_{H6-H5} = 7.9$	7.08 (tr)	$^4J_{H6-H8} = 1.0$ $^3J_{H6-H7} = 7.4$ $^3J_{H6-H5} = 7.9$	7.32 (tr)	$^4J_{H6-H8} = 1.0$ $^3J_{H6-H7} = 7.4$ $^3J_{H6-H5} = 7.9$
H6′	7.24 (dd)	$^3J_{H6'-H5'} = 8.4$ $^4J_{H6'-H2'} = 2.0$	7.21 (d)	$^3J_{H6'-H5'} = 8.4$ $^4J_{H6'-H2'} = 2.0$	7.00 (s)	– –
H2′	7.30 (d)	$^4J_{H6'-H2'} = 2.0$	7.26 (d)	$^4J_{H6'-H2'} = 2.0$	–	–
H7	7.52 (tr)	$^4J_{H7-H5} = 2.0$ $^3J_{H7-H6} = 6.9$ $^3J_{H7-H8} = 8.8$	7.56 (tr)	$^4J_{H7-H5} = 1.5$ $^3J_{H7-H6} = 7.4$ $^3J_{H7-H8} = 8.4$	7.61 (tr)	$^4J_{H7-H5} = 1.5$ $^3J_{H7-H6} = 7.4$ $^3J_{H7-H8} = 8.4$
H5	7.73 (dd)	$^4J_{H5-H7} = 2.0$ $^3J_{H5-H6} = 7.9$	7.75 (dd)	$^4J_{H5-H7} = 1.5$ $^3J_{H5-H6} = 7.9$	7.94 (dd)	$^4J_{H5-H7} = 1.5$ $^3J_{H5-H6} = 7.9$
Glu Hβ	1.68 (m)		1.81 (m)		1.53 (m)	
Glu Hγ	1.94 (m)		2.14 (m)		1.84 (m) 2.21 (m)	
Cys Hβ1	2.45 (dd)		2.26 (dd)		2.64 (dd) 2.95 (dd)	
Cys Hβ2	2.62 (dd)		2.66 (dd)		3.10 (dd) 3.23 (dd)	
Gly Hα1	3.32 (d)		3.31 (d)		3.30 (d)	
Gly Hα2	3.42 (d)		3.40 (d)		3.43 (d)	
Glu-Hα	3.55 (t)		3.50 (t)		3.38 (m)	
Cys Hα	3.96 (dd)		3.79 (dd)		3.77 (dd) 4.27 (dd)	

feasible, this isolated 5′-monoglutathionyl adduct was also incubated with HRP/H_2O_2 in the presence of GSH. As for the 2′-monoglutathionyl adduct, this resulted in the formation of a metabolite with the same retention time, the same UV spectrum, and the same mass and ^{1}H NMR characteristics as the metabolite identified as the 2′,5′-diglutathionyl taxifolin. Based on these data and arguments, we have assigned all diglutathionyl adducts as 2′,5′-diglutathionyl adducts.

Discussion

In the present study, the formation of glutathionyl adducts from a series of 3′,4′-dihydroxyflavonoid *o*-quinone/*p*-quinone methides was investigated with special emphasis on the regioselectivity of the GSH addition as a function of the pH. The flavonoid *o*-quinones were generated with the use of HRP, an enzyme shown before to catalyze the conversion of flavonoid catechols to their corresponding *o*-quinones (*11*, *12*). The GSH adducts were purified by HPLC and identified by LC/MS and ^{1}H and ^{13}C NMR analysis. Based on the quinone/quinone methide isomerization chemistry involved in the formation of the A ring type glutathionyl adducts from quercetin *o*-quinone/quinone methide (Figure 1), it can be postulated that especially the presence of the C2═C3 double bond, the C3−OH group, the C4−keto moiety, and the C5−OH group are required for efficient quinone methide formation and GSH adduct formation in the A ring instead of in the B ring. Furthermore, in our previous work, we have reported that especially for fisetin, regioselectivity and the nature of the quinone adducts formed appear to be dependent on the pH. Depending on pH, the site of GSH adduct formation shifted from the B ring to the C ring of fisetin (*18*). In the present study, the pH-dependent chemistry of flavonoid quinone/quinone methide chemistry was investigated in more detail using other flavonoid model compounds including the most widely studied flavonoid quercetin. This results in a new hypothesis describing the pH-dependent shift in the regioselectivity of GSH addition to the flavonoid quinone/quinone methides. Figure 8 schematically presents this model for quercetin.

With quercetin, at low pH, GSH is protonated (thiol form) and thus not nucleophilic enough to compete with the much more abundant water molecules. Water addition to the quercetin quinone/quinone methide takes place at C2═C3 in the C ring (Figure 8a) (*30*). This hydration results in 3,4-flavandione (I) as reported previously (*18*, *28*). In analogy with anthocyanins, a ring chain tautomeric equilibrium resulting in the chalcantrione (II) may exist, which subsequently leads to formation of the substituted 3(*2H*)-benzofuranone (III). Ultimately, GSH adds to the C═O group at C2 of compound III, resulting in formation of a set of two diastereoisomeric glutathionyl quercetin adducts in the C ring.

At neutral pH, GSH is partially present in its highly nucleophilic thiolate form, and GS^- addition is preferred over water addition. The quercetin *o*-quinone has lost its most acidic proton at 7-OH followed by an efficient mesomeric equilibrium of the quercetin *o*-quinone monoanion with its corresponding quinone methide isomers. Quinone methide formation in the A ring is thus favored, which gives rise to glutathionyl adduct formation in the A ring, leading to 6- and 8-glutathionyl quercetin adducts (Figure 8b) (*24*, *30*).

At alkaline pH, the quercetin *o*-quinone has lost its second most acidic proton at 3-OH, giving rise to its corresponding quinone dianion (*30*). The isomerization of quercetin *o*-quinone dianion to its corresponding *p*-quinone methide is hampered due to the second deprotonation step at 3-OH. As a result, the *o*-quinone form prevails, which result in GS^- conjugation in the B ring instead of in the A ring (Figure 8c).

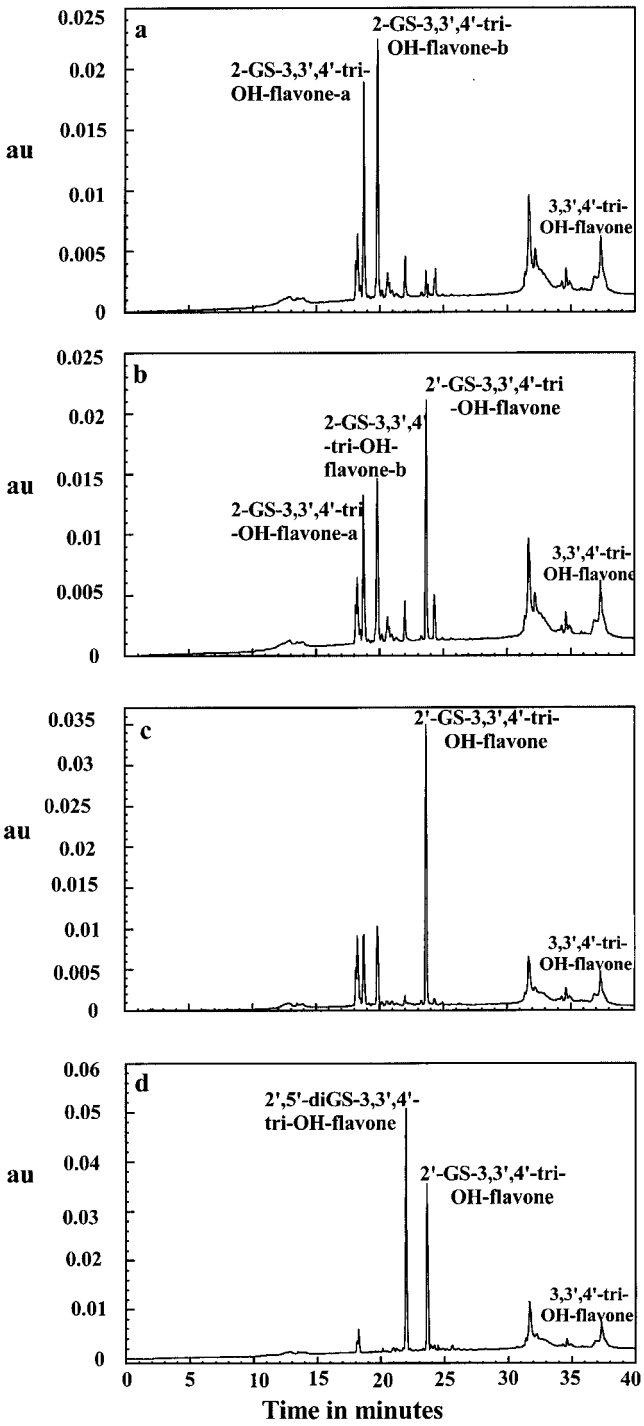

Figure 7. HPLC chromatograms of the incubation of 3,3′,4′-trihydroxyflavone with HRP in the presence of GSH at (a) pH 3.5, (b) pH 5.5, (c) pH 7.0, and (d) pH 8.5.

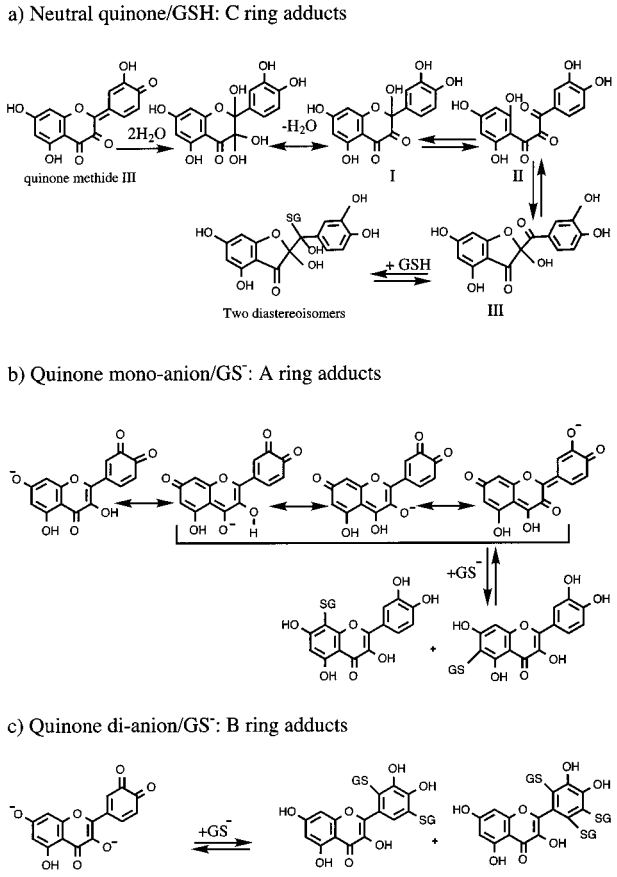

Figure 8. Schematic presentation of the mechanism for the pH-dependent formation of the glutathionyl/water adducts of quercetin quinone/quinone methide (a) at low pH, (b) at neutral pH, and (c) at alkaline pH. The deprotonation state and substituent pattern of the flavonoid quinone determine its quinone/quinone methide isomerization but also the regioselectivity of GSH addition.

With taxifolin and luteolin the absence of the C2═C3 double bond and/or the 3-OH group hampers the quinone methide isomerization of their *o*-quinone at all pH values and deprotonation states, and, thus, the GSH/GS⁻ addition is preferentially in the B ring. Formation of the 2′,5′-diglutathionyl adducts for both taxifolin and luteolin starts to occur when the concentration and reactivity of the 2′-monoglutathionyl adduct start to compete as substrate with the parent flavonoid, a process depending on its concentration and ionization potential (*18*). Thus, the major effect observed for the pH-dependent effect on HRP-mediated taxifolin and luteolin GSH/GS⁻ conjugation in the present study is on the rate of taxifolin and luteolin conversion and, as a result, on the ratio of mono- to diglutathionyl adduct formation.

In the case of fisetin (*18*), the absence of the 5-OH introduces a strong hydrogen bond between the C4═O keto and the C3−OH which also prevents isomerization to the quinone methide, thereby diminishing possibilities for A ring adducts. C ring addition, however, is still observed, probably not starting from the quinone methide III but, as previously indicated, from the quinone itself (*18*). Upon deprotonation of fisetin at alkaline pH, adduct formation in the B ring is observed as for all other flavonoid quinone/quinone methides. The pH-dependent chemistry of the quinone of 3,3′,4′-trihydroxyflavone is in line with what would be expected for the trihydroxyflavonoids based on Figure 8. Finally, the results of the present study elucidate the mechanism of the pH-dependent electrophilic behavior of B ring catechol flavonoids.

References

(1) Craft, K. D. (1998) The chemistry and biological effects of flavonoids and phenolic acids. *Ann. N.Y. Acad. Sci.* **854**, 435−442.

(2) Cody, V., Middleton, E., and Harborne, J. B. (1986) *Plant Flavonoids in Biology and Medicine: Biochemical Pharmacological and Structure−Activity Relationships*, A. R. Liss, New York.

(3) Middleton, E., Jr., and Kandaswami, C. (1993) The impact of plant flavonoids on mammalian biology: Implications for immunity,

inflammation and cancer. In *The flavonoids. Advances in Research Since 1986* (Harborne, J. H., Ed.) pp 619−652, Chapman and Hall, New York.
(4) Rice-Evans, C. A., Miller, N. J., and Paganga, G. (1996) Structure−antioxidant activity relationships of flavonoids and phenolic acids. *Free Radical Biol. Med.* **20**, 933−956.
(5) Jovanovic, S. V., Steenken, S., Tosic, M., Marjanovic, B., and Simic, M. G. (1994) Flavonoids as antioxidants. *J. Am. Chem. Soc.* **116**, 4846−4851.
(6) Hu, J. P., Calomme, M., Lasure, A., De Bruyne, T., Pieters, L., Vlietinck, A., and Vanden Berghe, D. A. (1995) Structure−activity relationships of flavonoids with superoxide scavenging ability. *Biol. Trace Elem. Res.* **47**, 327−331.
(7) Terao, J., Piskula, M., and Yao, Q. (1994) Protective effect of epicatechin, epicatechin gallate and quercetin on lipid peroxidation in phospholipid bilayers. *Arch. Biochem. Biophys.* **308**, 278−284.
(8) Morel, J., Lescoat, G., Cogrel, P., Sergent, O., Pasdeloup, N., Brissot, P., Cillard, P., and Cillard, J. (1993) Antioxidant and iron-chelating activities of the flavonoids catechin, quercetin and diosmetin on iron-loads rat hepatocyte cultures. *Biochem. Pharmacol.* **45**, 13−19.
(9) Bors, W., Heller, W., Michel, C., and Saran, M. (1990) Flavonoids as antioxidants: determination of radical-scavenging efficiencies. *Methods Enzymol.* **186**, 343−355.
(10) Laughton, M. J., Halliwell, B., Evans, P. J., and Hoult, J. R. S. (1989) Antioxidant and prooxidant actions of the plant phenolics quercetin, gossypol and myricetin. *Biochem. Pharmacol.* **38**, 2859−2865.
(11) Metodiewa, D., and Dunford, H. B. (1993) Medical aspects and techniques for peroxidases and catalases. In *Atmospheric Oxidation and Antioxidants* (Scott, G., Ed.) Vol. III, pp 287−332, Elsevier, Amsterdam.
(12) Metodiewa, D., Jaiswal, A. K., Cenas, N., Dickancaite, E., and Segura-Aguilar, J. (1999) Quercetin may act as a cytotoxic prooxidant after its metabolic activation to semiquinone and quinoidal product. *Free Radical Biol. Med.* **26**, 107−116.
(13) Canada, A. T., Giannella, E., Nguyen, T. D., and Mason, R. P. (1990) The production of reactive oxygen species by dietary flavonols. *Free Radical Biol. Med.* **9**, 441−449.
(14) Galati, G., Chan, T., Wu, B., and O'Brien, P. J. (1999) Glutathione-dependent generation of reactive oxygen species by the peroxidase-catalyzed redox cycling of flavonoids. *Chem. Res. Toxicol.* **12**, 521−525.
(15) O'Brien, P. J. (1988) Radical formation during the peroxidase-catalysed metabolism of carcinogens and xenobiotics: the reactivity of these radicals with GSH, DNA and unsaturated lipid. *Free Radical Biol. Med.* **4**, 169−183.
(16) Sudhar, P. S., and Armstrong, D. A. (1990) Redox potential of some sulfer containing radicals. *J. Phys. Chem.* **94**, 5915−5917.
(17) Galati, G., Moridani, M. Y., Chan, T. S., and, O'Brien, P. J. (2001) Peroxidative metabolism of apigenin and naringenin versus luteolin and quercetin: glutathione oxidation and conjugation. *Free Radical Biol. Med.* **30**, 370.
(18) Awad, H. M., Boersma, M. G., Boeren, S., Van Bladeren, P. J., Vervoort, J., and Rietjens, I. M. C. M. (2001) Structure−activity study on the quinone/quinone methide chemistry of flavonoids. *Chem. Res. Toxicol.* **14**, 398−408.
(19) Awad, H. M., Boersma, M. G., Vervoort, J., and Rietjens, I. M. C. M. (2000) Peroxidase-catalysed formation of quercetin quinone methide glutathione adducts. *Arch. Biochem. Biophys.* **378**, 224−233.
(20) Boersma, M. G., Vervoort, J., Szymusiak, H., Lemanska, K., Tyrakowska, B., Cenas, N., Segura-Aguilar, J., and Rietjens, I. M. C. M. (2000) Regioselectivity and reversibility of the glutathione conjugation of quercetin quinone methide. *Chem. Res. Toxicol.* **13**, 185−191.
(21) Primus, J.-L., Boersma, M. G., Mandon, D., Boeren, S., Veeger, C., Weiss, R., and Rietjens, I. M. C. M. (1999) The effect of iron to manganese substitution on microperoxidase 8 catalysed peroxidase and cytochrome P450 type of catalysis. *J. Biol. Inorg. Chem.* **4**, 274−283.
(22) Osman, A. M., Koerts, J., Boersma, M. G., Boeren, S., Veeger, C., and Rietjens, I. M. C. M. (1996) Microperoxidase/H_2O_2-catalysed aromatic hydroxylation proceeds by cytochrome-P-450-type oxygen-transfer reaction mechanism. *Eur. J. Biochem.* **240**, 232−238.
(23) Stoll, V. C., and Blanchard, J. S. (1990) Buffers: Principles and practice. *Methods Enzymol.* **182**, 24−38.
(24) Frey-Schröder, G., and Barz, W. (1979) Isolation and characterization of flavonol converting enzymes from *Mentha piperita* plants and from *Mentha arvensis* cell suspension cultures. *Z. Naturforsch.* **34C**, 200−209.
(25) Howard, P. H., Arlend, D. K., and Craig, E. L. (1994) Electrochemistry of catechol-containing flavonoids. *J. Pharm. Biomed. Anal.* **12**, 325.
(26) Corazza, A., Harvey, I., and Sadler, P. J. (1996) H-1, C-13-NMR and X-ray absorption studies of copper(I) glutathione complexes. *Eur. J. Biochem.* **236**, 697−705.
(27) Markham, K. R., and Geiger, H. (1993) ^{1}H NMR magnetic resonance spectroscopy of flavonoids and their glycosides in hexadeuteriodimethyl sulfoxide. In *The Flavonoids: Advances in Research Since 1986* (Harborne, J. H., Ed.) pp 619−652, Chapman and Hall, London.
(28) Jorgensen, L. V., Cornett, C., Justesen, U., Skibsted, L. H., and Dragsted, L. O. (1998) Two-electron electrochemical oxidation of quercetin and kaempferol changes only the flavonoid C-ring. *Free Radical Res.* **29**, 339−350.
(29) Aksnes, D. W., Standnes, A., and Andersen, O. M. (1996) Complete assignment of the ^{1}H and ^{13}C NMR spectra of flavone and its A-ring hydroxyl derivatives. *Magn. Reson. Chem.* **34**, 820−823.
(30) Dangles, O., Fargeix, G., and Dufour, C. (1999) One-electron oxidation of quercetin derivatives in protic and non protic media. *J. Chem. Soc., Perkin Trans.* **2**, 1387.

TX010132L